RAPID COMMUNICATIONS

PHYSICAL REVIEW B VOLUME 44, NUMBER 23 15 DECEMBER 1991-I

Nonthermal laser-induced recrystallization of amorphous silicon

Jeff Bailey and Eicke R. Weber
Department of Materials Science, University of California, Berkeley, California 94720

Jon Opsal and Allan Rosencwaig
Therma-Wave Incorporated, Fremont, California 94539

(Received 21 March 1991; revised manuscript received 13 September 1991)

Low-intensity laser illumination has been found to induce recrystallization of amorphous layers in ion-implanted silicon wafers. With the conditions used here, the temperature rise is much lower than that usually required for annealing of amorphous silicon. Therefore, this is an observation of recombination-induced *nonthermal* recrystallization of amorphous silicon layers.

Laser annealing of semiconductors has been a subject of great interest in recent years as a technique for controlled post-implant recrystallization and impurity activation.[1,2] Pulsed laser annealing (PLA) utilizes intense pulses of laser light ($\leq 10^{11}$ W/cm^2) for short periods of time (1–100 nsec), whereas continuous-wave (cw) laser annealing employs lower laser-power densities (10^6–10^8 W/cm^2) and longer anneal times ($\sim 10^{-3}$ sec). It is generally accepted that recrystallization of amorphous silicon occurs in PLA via rapid melting and recrystallization of surface layers, from time-resolved reflectivity measurements[3] and observed dopant redistribution during annealing.[4] Recrystallization of amorphous layers by cw laser illumination is believed to occur via thermally activated solid-phase epitaxy at temperatures below the melting point of silicon.[5] However, we will present evidence for recrystallization induced by a low-power cw laser in a commercial modulated optical reflectance (MOR) mapping system at a temperature well below that required for thermal recrystallization.

MOR measurements are a well-established method of nondestructive semiconductor-device and material characterization. The technique is mainly used in silicon-device processing to monitor implant dose in ion-implanted wafers prior to annealing.[6] The MOR signal (defined below) is a quantitative measure of the degree of lattice disorder resulting from physical damage, e.g., during ion implantation. It was observed during MOR measurements of highly implanted silicon wafers at Therma-Wave Inc. that the focused laser beam used in the MOR apparatus resulted in a marked decrease in optical reflectivity as the beam was scanned over the wafer surface. This paper presents results of a systematic study of this phenomenon, in which implanted wafers were illuminated with focused laser light and examined via transmission electron microscopy.

Modulated-optical-reflectance experiments were performed using a Therma-Probe^{TM} system, commercial equipment of Therma-Wave Inc. The Therma-Probe employs a 5.5-mW Ar laser pump beam which is intensity modulated (1 MHz) and focused to a spot of about 0.8-μm diameter on the material surface ($\leq 7\times10^5$ W/cm^2 absorbed). In semiconductors, the incident beam creates both thermal waves and electron-hole-plasma waves. These waves are detected by monitoring the optical reflectance of the material at the point of incidence of the pump beam with a colinear He-Ne laser probe beam, since both the temperature and plasma waves affect the refractive index of the semiconductor. The normalized modulated change in reflectivity $\Delta R/R$ is known as the MOR signal, which has been shown to be highly sensitive to the presence of lattice defects.[7]

The temperature and plasma waves created by the pump beam can be described by the following diffusion equations:

$$D_t\nabla^2 T(\bar{x},t) - \frac{\partial T(\bar{x},t)}{\partial t} = -D_t\frac{Q(\bar{x},t)}{\kappa}\,, \tag{1}$$

$$D_a\nabla^2 N(\bar{x},t) - \frac{N(\bar{x},t)}{\tau} - \frac{\partial N(\bar{x},t)}{\partial t} = -P(\bar{x},t)\,, \tag{2}$$

in which T is the temperature, N is the plasma density, κ is the thermal conductivity, τ is the plasma lifetime, D_t and D_a are the thermal and plasma diffusivities, and Q and P are the source terms. Three-dimensional solutions to these equations[8] show that for a modulated source, the modulated plasma concentration and temperature at the surface can be strongly affected by nonuniformities in material parameters D_a, D_t, and κ. This is the basis of MOR imaging systems, in which the sample is scanned under the beam. In particular, the MOR signal in silicon was shown to depend mainly upon D_a, from carrier scattering by both ionized impurities and dislocations.[9]

Surface damage from ion implantation in semiconductors consists of isolated point-defect clusters at low doses, while at higher doses the lattice damage can accumulate until the surface region, or a layer below the surface, becomes amorphous.[10] In any case annealing is required after implantation to remove the implantation damage and to ensure that the implanted dopants reside on substitutional sites and are electrically active. Many methods of annealing have been developed, which differ widely in the characteristic time and temperature necessary for recrystallization. Energy can be provided in the form of intense, subnanosecond pulses of laser light, or furnace anneals lasting on the order of hours.[11] Furthermore, the temperature at which recrystallization occurs can be highly variable, and may approach or exceed the melting point

of silicon.[3,12] For furnace thermal annealing, recrystallization temperatures near 550 °C are typically used.[11]

Samples used in our experiments were Czochralski-grown silicon wafers of ⟨100⟩ orientation, implanted at 120 KeV with arsenic ions at doses of 1×10^{14} and 5×10^{14} As/cm^2. After MOR scanning, dark lines were visible on the wafer surfaces where the laser beam had passed. Plan view and cross-sectional transmission electron microscopy (TEM) was performed on samples prepared by laser drawing sets of parallel lines on the wafer surfaces, and lapping and ion milling the samples until they were electron transparent. Plan view and cross-sectional TEM was performed on Philips 301 (bright-field images) and JEOL 200CX (high resolution) electron microscopes.

The TEM micrographs are shown in Figs. 1 and 2. The cross-sectional micrograph of the 1×10^{14}/cm^2 wafer [Fig. 1(a)] shows that the implantation has created a buried amorphous layer and that the laser has increased the thickness of the upper crystalline layer. At a dose of 5×10^{14}/cm^2 a surface amorphous layer has formed [Fig. 1(b)]. In this case the laser beam resulted in diffraction contrast near the surface. High-resolution microscopy (Fig. 2) reveals that this contrast is caused by recrystallized silicon in the amorphous matrix. One can see in the micrograph that the crystallites are highly defective, containing numerous twin planes and stacking faults, which one would expect in rapidly recrystallized material. The diffraction pattern indicates randomly oriented crystallites, which are visible in the image. The width of the recrystallized stripe is approximately 1000 Å.

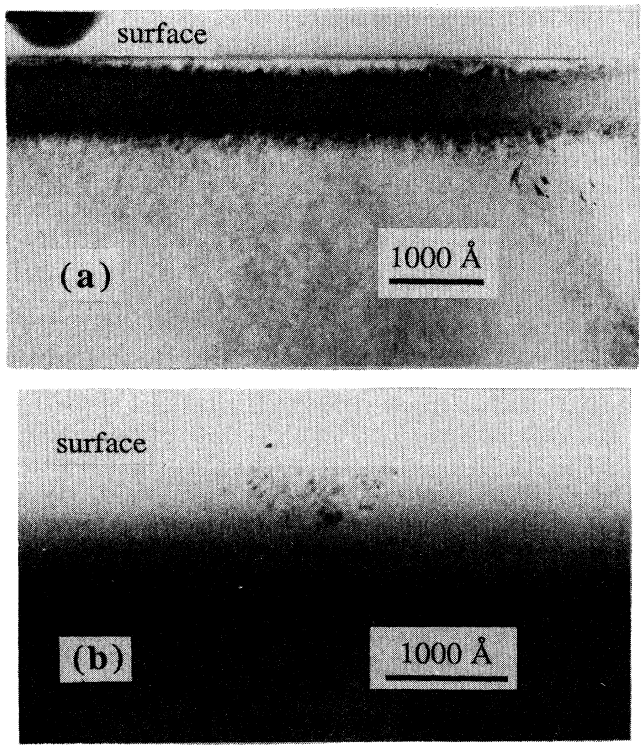

FIG. 1. Cross-sectional TEM micrographs of laser-illuminated wafers (5.5 mW laser intensity, 1 mm/sec scan speed). (a) 1×10^{14} As/cm^2; (b) 5×10^{14} As/cm^2.

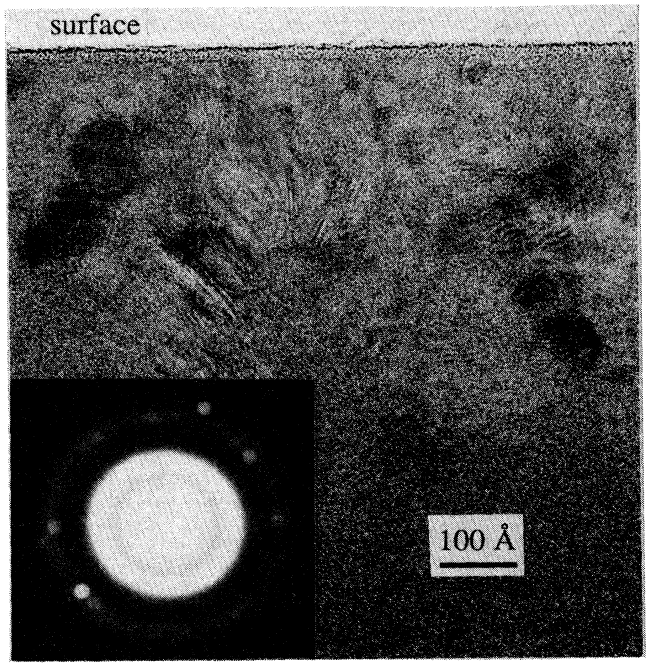

FIG. 2. High-resolution TEM micrograph of laser-illuminated 1×10^{14}/cm^2 wafer (5.5 mW laser intensity, 1 mm/sec scan speed).

Experiments were performed to determine the effect of changing Ar-laser power and scanning speed on this recrystallization-induced decrease in reflectivity. The decrease of optical reflectivity after focused laser illumination was found to be a function of both laser power and scan speed (see Figs. 3 and 4). Figure 3(b) shows that for the 5×10^{14}/cm^2 wafer (surface amorphous layer) there is a threshold of laser power above which the reflectivity de-

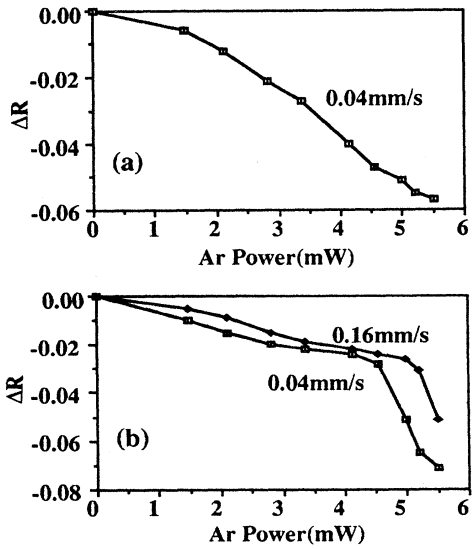

FIG. 3. Dependence of reflectivity change on Ar laser power (scan speeds indicated). (a) 1×10^{14}/cm^2; (b) 5×10^{14}/cm^2.

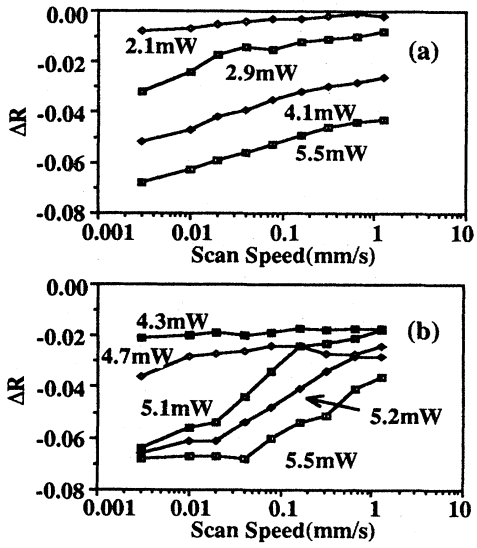

FIG. 4. Dependence of reflectivity change on laser scan speed (Ar laser powers indicated). (a) $1\times10^{14}/cm^2$; (b) $5\times10^{14}/cm^2$.

creases distinctly. A similar threshold of maximum scan speed is obvious for this type of sample, if the laser power is sufficiently high [Fig. 4(b)]. This threshold is not evident with the $1\times10^{14}/cm^2$ wafer (buried amorphous layer), for which the reflectivity change varies more smoothly with laser power and scan speed [Figs. 3(a) and 4(a)]. The total deposited energy for all scan speeds and attenuations ranges from about 2×10^2 to 2×10^5 J/cm^2.

Solutions of the electromagnetic wave equations show easily that the observed amorphous layer recrystallization can account quantitatively for the observed changes in reflectivity.

The recrystallization observed here was originally suspected to occur thermally via solid-phase epitaxy below the silicon melting temperature (1412 °C), since this has previously been demonstrated for cw annealing.[5,13] Using a relationship[14] for the dependence of maximum surface temperature and recrystallized thickness upon laser power, beam radius, and scan speed for a scanning cw laser on amorphous Si (based upon known thermal regrowth rates and solutions to the heat diffusion equations), we find that for the most intense irradiation (5.5 mW incident Ar laser, 0.8 μm beam diameter, 0.003 mm/sec scan speed), only a 20 °C maximum temperature increase under the laser beam can be expected, resulting in a recrystallized thickness of less than 10 Å. The experimentally known dependence of epitaxial regrowth rate on temperature [activation energy of 2.35 eV, $R_0=3.2\times10^{14}$ Å/sec for ⟨100⟩ (Ref. 14)] predicts that with the range of laser-exposure times used here (1–300 msec) the peak temperature would have to reach 600 °C to yield a recrystallized thickness of 100 Å. [Such a temperature is easily reached with the larger beam diameters used in previous cw annealing experiments,[5] even with an incident power density similar to that used here. The temperature increase is mainly a function[15] of (laser power)/(beam radius).] Calculations by the authors based on the three-dimensional thermal and plasma diffusion equations [Eqs. (1) and (2)] also show that the temperature increase directly under the beam is less than 50 °C.

Since the expected temperature increase is far from sufficient to account for thermal amorphous-layer regrowth, and considering the past successes of the thermal model for cw laser annealing,[5,13] we conclude that thermal recrystallization cannot be the cause for the effect observed here. An alternative to the thermal recrystallization model was proposed by Van Vechten and others.[16,17] The proposed "plasma annealing" (PA) model was originally based upon the idea that high plasma concentrations soften the covalent semiconductor bonds, greatly reducing the barrier for relaxation from the amorphous to the crystalline state. Although recombination-assisted defect migration is part of the PA model, nonlinearities in pulsed laser annealing suggested that ionization plays a greater part than recombination. The plasma concentration required to bring about this effect was believed to be about 8×10^{21} carriers/cm^3. Based on a three-dimensional solution to Eq. (2) the surface-plasma concentrations predicted for our experimental conditions are of the order of $3\times10^{19}/cm^3$, 2 orders of magnitude less than that expected to cause lattice instability. We believe, therefore, that the effect described here cannot be such a plasma-annealing process.

However, the high density of electron-hole pairs will result in recombination-enhanced defect migration. We propose that this phenomenon, which has been well documented for recombination-enhanced motion of point defects[18] and dislocations in semiconductors,[19] is the origin of this recrystallization effect. The amount of energy released by electron-hole recombination should be sufficient to initiate recrystallization. With a peak plasma density of $3\times10^{19}/cm^3$ and plasma lifetime of 10^{-8} sec, the maximum amount of energy available through electron-hole recombination is 7×10^8 J/sec cm^3; with the shortest laser dwell time of 1 msec, this corresponds to 7×10^5 J/cm^3, or about 80 eV/atom. The observed threshold in reflectivity change [Figs. 3(b) and 4(b)] for the $5\times10^{14}/cm^2$ implanted sample (surface amorphous layer) may simply be due to the fact that recrystallization is accelerated in the presence of an amorphous/crystalline interface; once recrystallization has been initiated within the amorphous layer, subsequent recrystallization proceeds more rapidly. In the case of the $1\times10^{14}/cm^2$ wafer (buried amorphous layer), no threshold exists because recrystallization is always epitaxial and rapid.

In summary, low-power laser illumination of silicon amorphous layers with a focused laser beam has been found to induce subthreshold recrystallization of amorphous silicon inducing a change in optical reflectivity. Recrystallization is confirmed by TEM. As the expected temperature rise for the illumination conditions used here is believed to be below 50 °C, it is concluded that carrier recombination in the dense electron-hole plasma is the cause of the observed recrystallization. This finding can have important consequences for the understanding of rapid thermal annealing processes, which might very well be enhanced significantly by recombination-enhanced defect motion.

[1]A. G. Cullis, Rep. Prog. Phys. **48**, 1155 (1985).
[2]I. W. Boyd and J. I. B. Wilson, Nature (London) **303**, 481 (1983).
[3]M. I. Nathan, R. T. Hodgson, and E. J. Yoffa, Appl. Phys. Lett. **36**, 512 (1980).
[4]J. C. Wang, R. F. Wood, and P. P. Pronko, Appl. Phys. Lett. **33**, 455 (1978).
[5]D. H. Auston *et al.*, Appl. Phys. Lett. **33**, 539 (1978).
[6]W. L. Smith, A. Rosencwaig, and D. L. Willenborg, Appl. Phys. Lett. **47**, 584 (1985).
[7]J. Bailey, E. Weber, and J. Opsal, in *Review of Progress in Quantitative NDE,* edited by D. O. Thompson and D. E. Chimenti (Plenum, New York, 1989), p. 1362.
[8]J. Opsal, A. Rosencwaig, and D. L. Willenborg, Appl. Opt. **22**, 3169 (1983).
[9]J. Bailey, E. R. Weber, and J. Opsal, J. Cryst. Growth **103**, 217 (1990).
[10]F. F. Morehead, B. L. Crowder, and R. S. Title, J. Appl. Phys. **43**, 1112 (1972).
[11]M. I. Current and K. A. Pickar, in *Proceedings of the Tutorial Symposium on Semiconductor Technology,* edited by D. A. Doane, D. B. Fraser, and D. W. Hess (Electrochemical Society, Pennington, NJ, 1982), p. 65.
[12]B. Stritzker, A. Pospieszczyk, and J. A. Tagle, Phys. Rev. Lett. **47**, 356 (1981).
[13]A. Gat *et al.*, Appl. Phys. Lett. **33**, 389 (1978).
[14]R. B. Gold and J. F. Gibbons, Mater. Res. Soc. Symp. Proc. **77**, 77 (1979).
[15]Y. I. Nissim *et al.*, J. Appl. Phys. **51**, 274 (1980).
[16]J. A. Van Vechten, R. Tsu, and F. W. Saris, Phys. Lett. **74A**, 422 (1979).
[17]*Semiconductors Probed by Ultrafast Laser Spectroscopy, Vol. 2,* edited by R. R. Alfano (Academic, New York, 1984).
[18]L. C. Kimerling, Solid State Electron. **21**, 1391 (1978).
[19]K. H. Küsters and H. Alexander, Physica B **116**, 594 (1983).

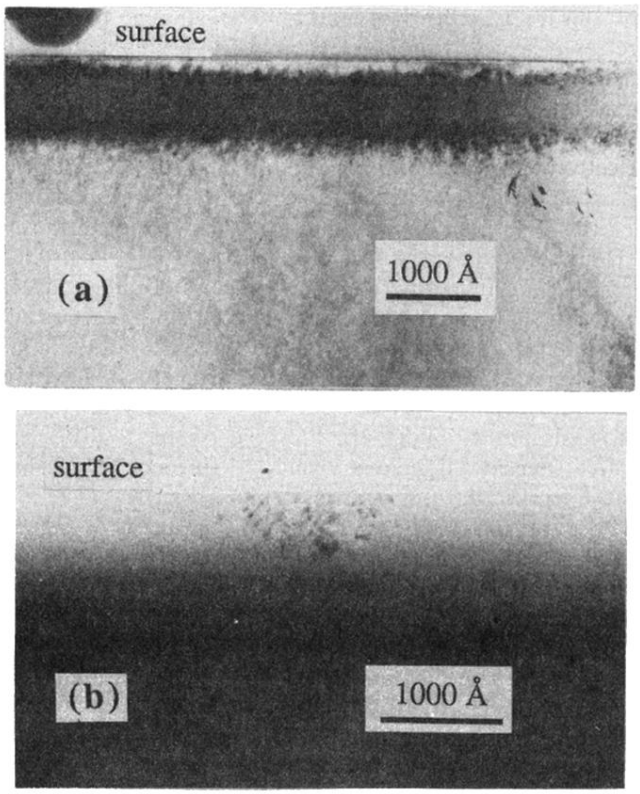

FIG. 1. Cross-sectional TEM micrographs of laser-illuminated wafers (5.5 mW laser intensity, 1 mm/sec scan speed). (a) 1×10^{14} As/cm^2; (b) 5×10^{14} As/cm^2.

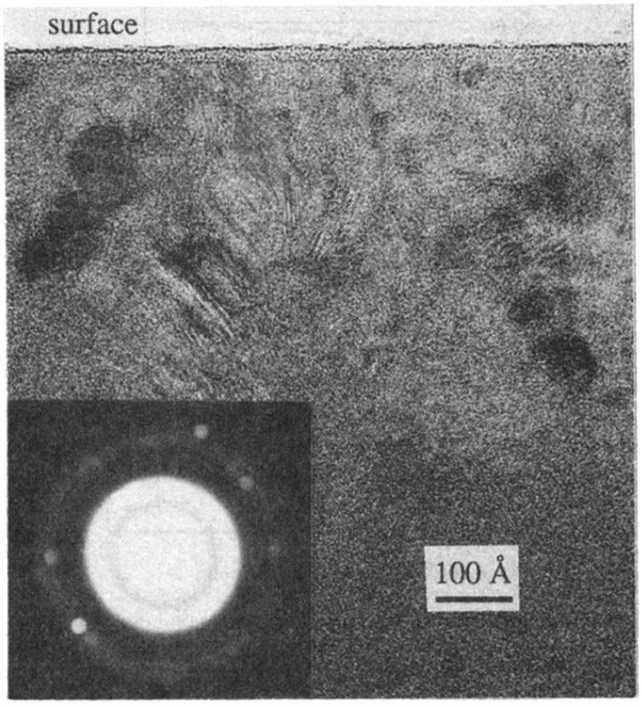

FIG. 2. High-resolution TEM micrograph of laser-illuminated $1 \times 10^{14}/cm^2$ wafer (5.5 mW laser intensity, 1 mm/sec scan speed).